Cyclical Changes in the Timing Residuals from the Pulsar B0919+06

Tatiana V. Shabanova

Pushchino Radio Astronomy Observatory, Astro Space Center, P. N. Lebedev Physical Institute, Russian Academy of Sciences, 142290 Pushchino, Russia

tvsh@prao.ru

ABSTRACT

We report the detection of a large glitch in the pulsar B0919+06 (J0922+0638). The glitch occurred in 2009 November 5 (MJD 55140) and was characterized by a fractional increase in the rotation frequency of $\Delta\nu/\nu \sim 1.3 \times 10^{-6}$. A large glitch happens in the pulsar whose rotation has unstable character. We present the results of the analysis of the rotation behavior of this pulsar over the 30-year time span from 1979 to 2009. These results show that the pulsar's rotation frequency underwent continuous, slow oscillations which look like glitch-like events. During the 1991–2009 interval, the pulsar experienced a continuous sequence of 12 slow glitches with a fractional increase in the rotation frequency $\Delta\nu/\nu \sim 1.5 \times 10^{-9}$. All the slow glitches observed have a similar signature related to a slow increase in the rotation frequency during $\sim$ 200 days and the subsequent relaxation back to the pre-glitch value during ~ 400 days. We show that a continuous sequence of such slow glitches is characterized by practically identical amplitudes $\Delta\nu \sim 3.5 \times 10^{-9}$ Hz and identical time intervals between glitches ~ 600 days and is well described by a periodic sawtooth-like function. The detection of two different phenomena, such as a large glitch and a sequence of slow glitches, indicates the presence of two types of discontinuities in the rotation frequency of the pulsar B0919+06. These discontinuities can be classified as normal and slow glitches.

Subject headings: pulsars: general — pulsars: individual (PSR B0919+06) — stars: neutron — stars: rotation

1. Introduction

The pulsar B0919+06 was discovered in the second Molonglo pulsar survey (Manchester et al. 1978). It has a period of 0.430 s, a period derivative of 13.72×10^{-15}, and a characteristic age

of $\tau = P/2\dot{P} \sim 5 \times 10^5$ years. A pulsar distance of 1200 pc and a transverse speed of 505 km s^{-1} were derived from the measurements of astrometric parameters (Chatterjee et al. 2001).

The data set analyzed includes the archival Jet Propulsion Laboratory (JPL) data and the Pushchino Radio Astronomy Observatory (PRAO) data. The early timing observations of PSR B0919+06 were carried out at the JPL at the frequency of 2388 MHz between 1979 December and 1983 March and covered a span of 3.2 years (Downs & Krause-Polstorff 1986). At the PRAO, timing observations of the pulsar were made between 1983 August and 2010 February. Together, both the data sets cover the 30-year span from 1979 to 2009 with a four-year gap between 1987 and 1990. An analysis of these experimental data showed that PSR B0919+06 has unstable rotation over the entire data span. The timing residuals after the removal of deterministic pulsar spin-down from the arrival times are characterized by a large second derivative that indicates a high level of timing noise.

Two types of unpredictable variations may occur in the spin rate of pulsars – timing noise and glitches (Shemar & Lyne 1996). Timing noise is manifestation of random, continuous wandering of the pulse phase that may produce long-term polynomial trends in the timing residuals. Glitches represent sudden, discrete jumps in the pulsar's rotation frequency, followed by an exponential recovery to the pre-glitch value. Glitches are characterized by short rise times of less than one day and reveal themselves as sudden discontinuities in the timing residuals.

A study of the timing behavior of the pulsars B1822−09 and B1642−03 has shown that there is another type of glitches which can be classified as peculiar or slow glitches (Shabanova 1998; Shabanova & Urama 2000; Zou et al. 2004; Shabanova 2005, 2007, 2009a,b, hereafter SH09). Characteristic features of slow glitches are long rise times of about 200–500 days and small amplitudes of about several parts in 10^{-9} Hz. Slow glitches produce cyclical changes in the timing residuals. The rotation frequency of these pulsars undergoes continuous, slow oscillations during a long period of time. For the pulsar B1822−09, the oscillatory changes in the rotation frequency were observed over the 1995–2004 interval. In the case of PSR B1642−03, cyclical changes in the timing residuals are observed during the 40-year period from 1969 to 2008. This pulsar demonstrates such striking properties of the slow glitches which allow us to predict the epochs and the amplitudes of new glitches in its rotation frequency (see SH09).

In this paper, we study the rotation history of the pulsar B0919+06 over the 30-year period, report the detection of a large glitch, and show that cyclical changes in the timing residuals from this pulsar are due to the presence of slow glitches. These results indicate that two types of discontinuities, specified as normal and slow glitches, can occur in the rotation frequency of one pulsar.

2. Observations and Timing Analysis

Timing observations of the pulsar B0919+06 were carried out at the Pushchino Observatory for more than 26 years from 1983 August to 2010 February with a four-year gap between 1987 and 1990. The observations were made with the Large Phased Array of the Pushchino Observatory, which is a transit telescope, at frequencies near 102 or 112 MHz using a 64-channel radiometer with a channel bandwidth of 20 kHz and a time resolution of 2.56 or 1.28 ms. The duration of one observation of PSR B0919+06 was determined by the width of the antenna beam at the pulsar declination and lasted 3.2 minutes. During this time, 450 individual pulses were summed synchronously with a predicted topocentric pulsar period to produce the mean pulse profile in each 20 kHz channel. After dispersion removal, all the channel profiles were summed to form an integrated pulse profile for the given observing session. Then this integrated profile was cross-correlated with a standard low-noise template to give the topocentric pulse arrival times for each observing session.

The topocentric arrival times collected at PRAO and the geocentric arrival times obtained from the archival JPL timing data were all referred to as the barycenter of the solar system at infinite frequency using the program TEMPO [1] and the JPL DE200 ephemeris. The position and the proper motion that are required for this correction were taken from Hobbs et al. (2004) and Chatterjee et al. (2001), respectively. In order to obtain residuals from the timing model, the pulsar's rotation is modeled by a polynomial including several frequency derivatives. In accordance with a Taylor expansion, the pulse phase φ at the barycentric arrival time t is expressed as:

$$\varphi(t) = \varphi_0 + \nu(t - t_0) + \dot{\nu}(t - t_0)^2/2 + \ddot{\nu}(t - t_0)^3/6..., \quad (1)$$

where φ_0, ν, $\dot{\nu}$, and $\ddot{\nu}$ are the pulse phase, rotation frequency, first and second frequency derivative at some reference time t_0, respectively. The timing residuals, obtained as differences between the observed times and the times predicted by a best fit model, were used for an analysis of the rotation behavior of the pulsar. The pulsar position was held fixed in the fitting procedure.

In order to study variations in the pulsar's rotation, the parameters ν and $\dot{\nu}$ were calculated from the local fits, performed to the pulse arrival times over the intervals of 150 or 300 days. The frequency residuals $\Delta\nu$ were obtained at the initial epoch of each interval relative to a third-order polynomial (1), including the mean parameters ν, $\dot{\nu}$, and $\ddot{\nu}$ defined over the full interval 1979–2009, 1991–2009 or any other interval.

[1] http://www.atnf.csiro.au/research/pulsar/tempo

3. Results

3.1. A Large Glitch of 2009

In 2009 November 5, the pulsar B0919+06 suffered a very large glitch with the fractional increase in the rotation frequency $\Delta\nu/\nu = 1.3\times10^{-6}$. This glitch is comparable in size to the glitches observed in the Vela pulsar. The glitch was accompanied by a significant decrease in the frequency derivative $\Delta\dot{\nu}/\dot{\nu} = -7\times10^{-3}$. A glitch was detected during a series of daily observations, so the uncertainty in determining the glitch epoch was within several hours, MJD 55139.8(1). Figure 1 shows the timing residuals relative to a simple ν, $\dot{\nu}$ model fitted to the data before the glitch. The negative growth in the residuals due to this glitch corresponds to a shift of the pulse in the observing window by $\sim$ 109 ms/day. The glitch parameters are given in Table 1. Uncertainties in parentheses represent the formal standard deviation and refer to the last digit quoted.

The large glitch has occurred in a relatively old pulsar with a characteristic age of $\tau \sim 5\times10^5$ years. This age is comparable to the age of PSR B0355+54 ($\tau \sim 5.6\times10^5$ years) that experienced a giant glitch with $\Delta\nu/\nu = 4.4\times10^{-6}$ in 1987 (Lyne 1987). The timing observations of PSR B0919+06 over four months after the glitch are not sufficient for the detailed research of the post-glitch behavior. Moreover, as will be shown in the following sections, the rotation frequency of this pulsar undergoes continuous, slow oscillations with the spacing of maxima $\sim$ 600 days. Further observations are needed to establish a relationship between the large glitch and this oscillatory behavior.

3.2. The Timing Behavior of the Pulsar Between 1979 and 2009

The timing behavior of PSR B0919+06 over the 30-year interval from 1979 December to 2009 November before the large glitch occurred is presented in Figure 2. A four-year data gap seen in the residuals between 1987 and 1990 insignificantly distorts the information about the pulsar's rotation.

An analysis of the full data set showed that the timing behavior of PSR B0919+06 exhibits significant deviations from a deterministic spin-down low that indicates a presence of large timing noise. So, the pulsar's rotation was modeled by polynomials including several frequency derivatives. The timing residuals after subtraction of the third-order polynomial for ν and two frequency derivatives $\dot{\nu}$ and $\ddot{\nu}$ are shown in Figure 2(a). The corresponding rotation parameters for the model 1979–2009 are given in Table 2. The post-fit residuals display a large quartic term with the amplitude approximately equal to half the pulsar

period. This plot shows that the residual curve has weak but well noticeable short-term cyclical structure over the entire time span.

This cyclical structure become more discernible in the timing residuals presented in Figure 2(b). The post-fit residuals obtained after subtraction of a polynomial including ν and three frequency derivatives exhibit the three maxima of a large-scale structure. The timing model with higher-order derivatives, for example, with four or five frequency derivatives, gives similar post-fit residuals and does not remove this structure from the timing residuals. Its origin is uncertain. We pay attention to the short-term cyclical structure superimposed on this residual curve. It contains 19 cycles which are located through the intervals approximately equal to 600 days. The properties of just this cyclical structure will be studied in detail in the following sections.

The changes in the rotation frequency with time are shown in Figure 2(c). The curve A marks the frequency residuals $\Delta\nu$ relative to the mean rotation parameters ν, $\dot{\nu}$, and $\ddot{\nu}$ over the 1979–2009 interval (Table 2). The values of ν were calculated from the local fits, performed to the pulse arrival times over the intervals of $\sim$ 300 days. This interval is approximately equal to half a cycle duration in the timing residuals. The strong curvature of the $\Delta\nu$ curve is due to the presence of higher-order frequency derivatives which are not taken into account by the timing model.

The curve A clearly shows that the signature of the frequency residuals $\Delta\nu$ has a sawtooth-like character. This pattern is well appreciable over the interval 1991–2009. The observed appearance of the $\Delta\nu$ changes indicates that the rotation frequency of the pulsar underwent slow oscillations during all the observational interval. These slow oscillations in ν give rise to cyclical changes in the timing residuals. Our purpose is to determine the cause of slow oscillations in the pulsar's rotation frequency. Because of the paucity of data between 1979 and 1986, the properties of this oscillatory structure will be investigated over the time span from 1991 to 2009 where there is a great deal of experimental data.

3.3. Slow Oscillations in the Pulsar's Rotation Frequency over the Interval 1991–2009

Figure 3 exhibits the timing behavior of the pulsar over the 19-year period between 1991 January and 2009 November. Figure 3(a) displays the timing residuals after subtraction of a polynomial including ν and two frequency derivatives. The rotation parameters measured over this period are given in Table 2. The last point in the residual curve indicates the large glitch that occurred in 2009 November 5. The short-term cyclical structure is clearly seen

in the timing residuals.

The timing residuals after subtraction of a polynomial including ν and five frequency derivatives are given in Figure 3(b). This plot shows a clear cyclical structure that contains 12 cycles with the amplitudes of about 10 ms and the spacing of maxima of about 600 days. Comparison of the timing residuals presented in Figures 2(a) and 2(b) and Figures 3(a) and 3(b) exhibits that the epochs and the spacing of the maxima of these cycles are the same in all the plots and do not depend on the time span of the data analyzed and the polynomial model fitted. At the same time, the shape and amplitude of these cycles are different in these plots.

The time behavior of the frequency residuals $\Delta\nu$ and the frequency derivative $\dot{\nu}$ relative to the mean rotation parameters for the model 1991–2009 from Table 2 are presented in Figures 3(c) and 3(d). The plotted values of ν and $\dot{\nu}$ were calculated from the local fits, performed to arrival time data over the intervals of ~ 150 days that overlapped by 75 days. Then the eight points in $\Delta\nu$ will correspond to a cycle duration of 600 days in the timing residuals.

It is clearly seen from Figure 3(c) that the rotation frequency of the pulsar B0919+06 slowly oscillates during the time interval observed. In each successive cycle, the stage of increase in $\Delta\nu$ is followed by the stage of decrease in $\Delta\nu$. This oscillatory process looks like a continuous sequence of 12 glitch-like events. In contrast to normal glitches, these events can be classified as peculiar or slow glitches because they exhibit long rise times of about a few hundred days. The similar glitch phenomenon was observed earlier in the pulsar B1642−03 (see SH09). Figure 3(d) shows that the time changes in the frequency derivative $\dot{\nu}$ are the effect of the changes in $\Delta\nu$. The peaks of $\Delta\dot{\nu}$ define the steepness of the front in the $\Delta\nu$ cycles. In order to study the properties of the slow glitches observed, it is necessary to obtain the shape of the $\Delta\nu$ cycles which is not distorted by the presence of the timing noise.

3.4. The Properties of the Slow Glitches Observed

From Figure 3(c), it is seen that the $\Delta\nu$ curve shows appreciable deviations relative to the timing model 1991-2009. These deviations are a result of the variations in $\dot{\nu}$ due to higher-order frequency derivatives which are not taken into account by the timing model. In order to obtain the undistorted shape of the $\Delta\nu$ cycles, we should calculate the frequency residuals $\Delta\nu$ relative to several timing models that describe the data over the shorter time intervals, including a few slow glitches. A measured magnitude of $\ddot{\nu}$ is so large that a simple ν, $\dot{\nu}$ spin

down model cannot be used to describe the experimental data even over the short intervals. Besides, $\ddot{\nu}$ changes a sign within the interval 1991–2009. The positive value $\ddot{\nu} = 1.6 \times 10^{-25} s^{-3}$ measured over the interval 1991–2002 becomes negative $\ddot{\nu} = -4.1 \times 10^{-25} s^{-3}$ over the next interval 2002–2009. The maximum length of each short time interval was determined by such quantity of the $\Delta\nu$ cycles that the timing residuals relative to the model, including the mean values of ν, $\dot{\nu}$, and $\ddot{\nu}$ defined over this interval, were nearly symmetrical with respect to the X-axis.

We found the three suitable time intervals on which the pulse arrival times, corresponding to a few slow glitches, are well described by the ν, $\dot{\nu}, \ddot{\nu}$ model. The timing model 1991-1995 was used to define the frequency residuals $\Delta\nu$ for glitches 1, 2, 3, and 4; the model 1995-2004 – for glitches 5, 6, 7, and 8; the model 2004–2009 – for glitches 9, 10, 11, and 12. The frequency residuals $\Delta\nu$ defined relative to these three models were combined then into a single data set. This adjusted set of the $\Delta\nu$ cycles describing the shape of 12 slow glitches is plotted in Figure 4(a). It is seen that the $\Delta\nu$ curve is nearly symmetrical with respect to the zero line. This indicates that the shapes of the slow glitches were reconstructed rather correctly (compare with Figure 3(c)).

The parameters describing the sequence of 12 slow glitches plotted in Figure 4(a) are given in Table 3. The parameters are presented in the following order: the glitch number; epoch of the point T_{min}, which corresponds to the minimum deviation of $\Delta\nu_{min}$; epoch of the point T_{max}, which corresponds to the maximum deviation of $\Delta\nu_{max}$; the glitch amplitude $\Delta\nu_g = \Delta\nu_{max} + |\Delta\nu_{min}|$; the time interval to the next glitch ΔT_{max}; the time interval between the minimal points of the $\Delta\nu$ cycles ΔT_{min}; the rise time interval $\Delta T_{ris} = T_{max} - T_{min}$; the relaxation time interval after the glitch $\Delta T_{rel} = T_{min} - T_{max}$.

Figure 4(a) and Table 3 allow us to study the properties of the slow glitches in the dependence on the glitch number. The results are presented in Figure 5. The top panel of Figure 5 shows the relation between the glitch amplitude and the glitch number. It is seen that all the slow glitches have approximately an identical amplitude equal to $3.5(0.5) \times 10^{-9}$ Hz, where the error in parentheses is the formal standard deviation. The middle panel shows the relation between the time intervals ΔT_{max} (the interval between the successive glitches) and ΔT_{min} (the interval between the minimal points of the $\Delta\nu$ cycles) and the glitch number. This plot shows that the indicated intervals are approximately equal to 580 and 600 days, respectively. The bottom panel shows the relation between the glitch parameters ΔT_{rel} (the relaxation time interval) and ΔT_{ris} (the rise time interval) and the glitch number and defines the average values of these parameters equal to 400 and 180 days, respectively.

These three relations indicate that all the slow glitches observed have similar properties which can be described by the following average parameters. The glitches have a small

absolute amplitude equal to 3.5×10^{-9} Hz. They are characterized by the identical inter-glitch intervals ΔT_{max} and approximately the same width of the intervals ΔT_{min}, equal to $\sim$ 600 days. The glitches have similar signature related to a slow increase in the rotation frequency during $\sim$ 200 days and the subsequent relaxation back to the pre-glitch value during $\sim$ 400 days. The relaxation after all the glitches can be described by a linear curve as is seen from Figure 4(a). These properties suggest that the sequence of the slow glitches observed can be approximated by a sawtooth-like function.

We created the model sawtooth-like curve using the indicated average parameters. This model curve has the starting point MJD 48350 and includes 10 cycles consisting of two stages – the stage of a linear glitch arising with a timescale of 200 days and the stage of a linear post-glitch relaxation with a timescale of 400 days. Only two glitches observed, 2 and 3, take off from this sequence. An analysis of the $\Delta\nu$ cycles showed that event 2 represents the sum of two partially overlapping glitches 2 and 3. Glitch 3 defines the starting point of a new phase in the sequence of the slow glitches. Therefore, event 2 should be described by three stages – the stage of a linear glitch arising with a timescale of 200 days is followed by the stage in which the glitch amplitude keeps constant within 400 days (the duration of this interval corresponds to the duration of the relaxation time interval ΔT_{rel}) and only then is followed by a linear post-glitch relaxation with a timescale of 400 days. The derived values for this model sawtooth-like curve are given in Table 4.

Figure 4(b) shows a model sawtooth-like curve with a period of 600 days which is superimposed on the glitch sequence observed. It is seen that the maxima of the model curve well coincide with the maxima of nearly all the slow glitches. Only the maxima of glitches 8 and 9 slightly do not correspond to the model curve. However, as is seen from the plot, the slight deviations of the amplitude and phase of these cycles from a model curve do not change a phase of the next cycles of the sequence. Probably, the shape of these glitches was not restored precisely. The model curve very well describes partially overlapping glitches 2 and 3. It is seen that in this range there was a phase shift for 400 days, exactly equal to ΔT_{rel}. After that, point 3 started marking the starting point of a new phase in the sequence of the slow glitches. Despite the phase shift between points 2 and 3, we suppose that the model sawtooth-like function is a periodic function. A comparison of the model parameters T_{min} and T_{max}, given in Table 4, and the same experimental parameters, listed in Table 3, shows that these parameters agree well within a precision limited by the time resolution of $\sim$ 100 days. We conclude that a model periodic sawtooth-like function approximates a sequence of the slow glitches observed very well. This result indicates a surprising regularity in the occurrence of slow glitches – the time intervals between the slow glitches, equal to 600 days, keep constant within approximately of 100 days during $\sim$ 19 years.

Thus, we found that the cause of slow oscillations in the rotation frequency of PSR B0919+06 over the 1991–2009 interval lies in a continuous generation of slow glitches. The originality of these slow glitches is that they have similar properties and their sequence is described by a periodic sawtooth-like function. Estimates show that the time intervals between glitches remain constant within 100 days during ~ 19 years. The regular occurrence of similar slow glitches creates the sawtooth-like pattern in the frequency residuals with a period of 600 days. The presence of the regular pattern over a long time-span of 19 years indicates that the slow glitches observed are not random events.

This conclusion is also valid for the full time span 1979–2009. Figure 2(c) displays the curve B which represents the model sawtooth-like curve extended by an initial data segment 1979–1986. Poor and irregular experimental points obtained over this interval give an approximate picture of oscillations observed in the frequency residuals $\Delta\nu$ and the timing residuals. Nevertheless, as is seen in Figures 2(b) and 2(c), the cycles in the model sawtooth-like curve B correspond well to cyclical changes in the frequency and timing residuals. The curve B shows how cyclical changes in the rotation frequency could look if the pulsar's rotation was described by a simple spin-down model over the interval 1979–2009.

4. Summary

An analysis of the rotation behavior of the pulsar B0919+06 over the 30-year period from 1979 to 2009 has shown that the nature of cyclical changes in the timing residuals from this pulsar implies a continuous generation of slow glitches which have similar properties. They are characterized by small sizes of 3.5×10^{-9} Hz, long rise times of 200 days, and relaxation time intervals of 400 days. We found that a sequence of the slow glitches observed over the 1991-2009 interval is well approximated by a periodic sawtooth-like function with a period of 600 days. Estimates show that the time intervals between the slow glitches observed keep constant within approximately 100 days during this period. In Figure 2(c), the curve B suggests that this conclusion can be generalized to all the observational interval 1979–2009. We may suppose that a sequence of similar slow glitches occurring at regular time intervals produced a sawtooth-like modulation of the rotation frequency, superimposed on the secular spin down, during all the period 1979–2009. An analysis of the pulse arrival times showed that the process, responsible for a generation of the slow glitches over ~ 30 years, was interrupted by the large glitch of magnitude $\Delta\nu/\nu = 1.3 \times 10^{-6}$ that occurred in 2009 November 5.

5. Discussion

Slow glitches as a unique glitch phenomenon were originally detected for the pulsar B1822−09 in the timing observations which are carried out at the Pushchino radio telescope since 1991 (Shabanova 1998). Further observations showed that this pulsar experienced a series of five slow glitches and also suffered three glitches of normal signature (Shabanova & Urama 2000; Zou et al. 2004; Shabanova 2005, 2007, 2009a; Yuan et al. 2010). The slow glitches observed were characterized by a gradual increase in the rotation frequency with a long rise time of 100–300 days. It was found that all these slow glitches were the components of one process that acted continuously during $\sim$ 10 years from 1995 to 2004. Then these events were followed by two glitches of normal signature. The glitches of magnitude $\Delta\nu/\nu = 6.7 \times 10^{-9}$ and $\Delta\nu/\nu = 121 \times 10^{-9}$ occurred in 2006 January and 2007 January, respectively (Shabanova 2009a). All these events clearly show the presence of two types of discontinuities in the rotation frequency of the pulsar B1822−09. These discontinuities can be classified as normal and slow glitches.

The pulsar B1642−03 is the second pulsar known, after PSR B1822-09, in the rotation frequency of which slow glitches were revealed. As shown in SH09, the rotation frequency of this pulsar undergoes continuous generation of slow glitches and over the 40-year period of observations this pulsar suffered eight slow glitches. The amplitude of these glitches and the time interval to the next glitch obey a clear linear relation. This dependence gives strong evidence against the statement that slow glitches can be caused by the same process as the timing noise in pulsars (Hobbs et al. 2010). The existence of the modulation process which causes the discrete changes of the glitch amplitudes and the post-glitch time intervals in the dependence on the serial number of the glitch in a given modulation period also confirms that the slow glitches observed are the distinct events. The indicated dependencies allow us to predict the epochs and sizes of new glitches in this pulsar. The verification of these predictions can be obtained in the near future, in 2013. This verification will provide strongest evidence that the slow glitches observed are a unique glitch phenomenon.

The pulsar B0919+06 is the third pulsar in our research that experienced slow glitches in its rotation frequency. The main properties of slow glitches observed are a similarity in their signatures and a regularity in their occurrence. The regular occurrence of similar slow glitches produces a periodic sawtooth-like modulation of the rotation frequency with a period of 600 days. As discussed above, the timing residuals do not show strictly periodic cyclical changes because this pulsar possesses a high level of timing noise and the observed amplitude and the shape of the cycles depend on a polynomial model fitted. A derived sawtooth-like modulation of the rotation frequency, shown in Figure 2(c) by the curve B, is a result of reconstruction of cyclical changes that could take place in the pulsar's rotation frequency

if the pulsar rotation is modeled by a simple spin down model. The curve B reflects the properties of an actual process that generated slow glitches during ~ 30 years. This process was interrupted by a large glitch that occurred in 2009 November. The pulsar B0919+06, as well as B1822−09, clearly exhibits that the pulsar's rotation frequency underwent two types of discontinuities that can be classified as normal and slow glitches.

Comparison of the rotation parameters for the pulsars showing the slow glitches is presented in Table 5 where the pulsars are listed in order of decreasing of their age. The table gives the pulsar's B1950 name, the rotation parameters ν, $\dot{\nu}$, and $\ddot{\nu}$, characteristic age $\tau = P/2\dot{P}$, and surface magnetic field $B = 3.2\times10^{19}(P\dot{P})^{1/2}$ G. It is seen that all these pulsars are relatively old pulsars with ages greater than $\sim 10^5$ years. The oldest pulsar B1642−03 has only the slow glitches. Their amplitude and the time interval between glitches strictly obey a certain law, that is, the glitch sequence in this pulsar possesses the predicted, steady-state properties. The two others, B0919+06 and B1822−09, are substantially younger, have the higher frequency derivatives $\dot{\nu}$ and $\ddot{\nu}$, and the stronger magnetic fields. They experience large glitches of normal signature that followed the oscillatory process in the rotation frequency identified with slow glitches. A comparison of the pulsar parameters in this table indicates that a tendency to have a sequence of slow glitches with steady-state properties is correlated with the characteristic age of the pulsar. Probably, the number of pulsars with slow glitches in their rotation frequency will considerably increase in the future. The candidates can be pulsars that exhibit cyclical changes in the timing residuals.

Long sequences of the timing residuals were recently published for 366 pulsars observed at the Jodrell Bank between 1968 and 2006 (Hobbs et al. 2010). A detailed analysis of these data shows that the timing residuals of some pulsars have clear cyclical changes during all the period of observations. According to Hobbs et al. (2010), the quasi-periodic structure in the timing residuals is clearly visible for six pulsars: B1540−06, B1642−03, B1818−04, B1826−17, B1828−11, and B2148+63. It should be noted that all these pulsars are old pulsars with ages varying from 1×10^5 to 3.5×10^7 years. Among these pulsars there are two pulsars B1642−03 and B1828−11 that were investigated earlier. The results of spectral analysis by Hobbs et al. (2010) for these two pulsars agree with the results of previous papers (Stairs et al. 2000; Shabanova et al. 2001). It is known that clear periodic structure in the timing residuals of B1828−11 that is accompanied by correlated pulse shape changes is explained by free-precession of the neutron star (Stairs et al. 2000). In the case of PSR 1642−03, multiple low frequency components in the power spectrum of timing residuals can be explained well as a result of continuous generation of slow glitches, the amplitude of which is correlated with the time interval following the glitch (Shabanova 2009b).

As reported by Yuan et al. (2010), the slow glitches have been identified yet for two

pulsars J0631+1036 and B1907+10. The first pulsar is a young pulsar with $\tau \sim 4.4 \times 10^4$ years, and the second one is substantially older with $\tau \sim 1.7 \times 10^6$ years. The latter has cyclical timing residuals, as is shown in Figure 3 of Hobbs et al. (2010), that can imply cyclical changes in the rotation frequency.

It is thought that pulsar glitches reflect a variable coupling between the solid crust of a neutron star and the superfluid interior rotating more rapidly than the solid crust. In terms of vortex pinning models, the origin of glitches can be explained by the catastrophic unpinning of superfluid vortices (Anderson & Itoh 1975; Alpar et al. 1984, 1989, 1993; Pines & Alpar 1985). These models provide a satisfactory interpretation of large glitches in pulsars.

Now the interpretation of a phenomenon of slow glitches is uncertain. According to Hobbs et al. (2010), the slow glitch phenomenon is a quasi-periodic component of timing noise, unrelated to normal glitches. At the same time, the slow glitches revealed in PSR B1642−03 possess the properties which meet the requirements of the glitch models: 1) all the slow glitches observed have significant exponential decay after glitch which is characterized by the same parameter $Q \sim 0.9$, 2) the size of glitches and the time interval to the following glitch obey a strong linear relation. The third property, the presence of a modulation process which forces the glitch amplitudes and the inter-glitch intervals to change with a discrete step, was not considered yet by any theory of pulsar glitches. In the case of slow glitches, it is necessary to account for the cause of a continuous generation of slow glitches.

For PSR B0919+06, a sawtooth-like modulation of the rotation frequency with a period of 600 days could be interpreted by the free precession of an isolated pulsar if this modulation was accompanied by correlated observable changes in the pulse profile (Shaham 1977; Nelson et al. 1990; Cordes 1993; Stairs et al. 2000). We detected no pulse profile changes during our observations at 112 MHz. A precession model requires a strictly periodic modulation of the pulsar's rotation frequency. The presence of the phase shift, equal to 400 days, in the modulation curve B between cycles 9 and 10, as is shown in Figure 2(c), contradicts this requirement. These two arguments testify against the interpretation of this sawtooth-like modulation in the terms of a free precession model. Besides, this pulsar has experienced a large glitch. As discussed by Link (2007), a slowly precessing neutron star cannot produce a glitch. The useful information for explanation of an origin of slow glitches can be obtained from further timing observations of PSR B0919+06. The observations in the nearest 5–10 years allow us to find out whether there is a relationship between different phenomena observed in this pulsar, such as a large glitch and a sequence of the slow glitches. Whether a large glitch has put a stop to a process of generation of slow glitches or this process continues to work after a large glitch in the same mode.

I should like to thank R. D. Dagkesamansky for useful discussion and comments, the staff of the PRAO for their aid in carrying out the many-year observations of this pulsar on the LPA antenna. This work was supported by the European Commission 6th Framework Program, Square Kilometre Array Design Studies (SKADS project, contract no. 011938) and the Russian Foundation for Basic Research (grant 09-02-00473).

REFERENCES

Alpar, M. A., Anderson, P. W., Pines, D., & Shaham, J. 1984, ApJ, 276, 325

Alpar, M. A., Chau, H. F., Cheng, K. S., & Pines, D. 1993, ApJ, 409, 345

Alpar, M. A., Cheng, K. S., & Pines, D. 1989, ApJ, 346, 823

Anderson, P. W., & Itoh, N. 1975, Nature, 256, 25

Cordes, J. M. 1993, in ASP Conf. Ser. 36, Planets around Pulsars, ed. J. A. Phillips, S. E. Thorsett, & S. R. Kulkarni (San Francisco, CA: ASP), 43

Chatterjee, S., Cordes, J. M., Lazio, T. J. W., Goss, W. M., Fomalont, E. B., & Benson, J. M. 2001, ApJ, 550, 287

Downs, G. S., & Krause-Polstorff, J. 1986, ApJS, 62, 81

Hobbs, G., Lyne, A. G., & Kramer, M. 2010, MNRAS, 402, 1027

Hobbs, G., Lyne, A. G., Kramer, M., Martin, C. E., & Jordan, C. 2004, MNRAS, 353, 1311

Link, B. 2007, Ap&SS, 308, 435

Lyne, A. G. 1987, Nature, 326, 569

Manchester, R. N., Lyne, A. G., Taylor, J. H., Durdin, J. M., Large, M. I., & Little, A. G. 1978, MNRAS, 185, 409

Nelson, R. W., Finn, L. S., & Wasserman, I. 1990, ApJ, 348, 226

Pines, D., & Alpar, M. A. 1985, Nature, 316, 27

Shabanova, T. V. 1998, A&A, 337, 723

Shabanova, T. V. 2005, MNRAS, 356, 1435

Shabanova, T. V. 2007, Ap&SS, 308, 591

Shabanova, T. V. 2009a, Astron. Rep., 53, 465

Shabanova, T. V. 2009b, ApJ, 700, 1009 (SH09)

Shabanova, T. V., Lyne, A. G., & Urama, J. O. 2001, ApJ, 552, 321

Shabanova, T. V., & Urama, J. O. 2000, A&A, 354, 960

Shaham, J. 1977, ApJ, 214, 251

Shemar, S. L., & Lyne, A. G. 1996, MNRAS, 282, 677

Stairs, I. H., Lyne, A. G., & Shemar, S. L. 2000, Nature, 406, 484

Yuan, J. P., Wang, N., Manchester, R. N., & Liu, Z. Y. 2010, MNRAS, 404, 289

Zou, W. Z., Wang, N., Wang, H. X., Manchester, R. N., Wu, X. J., & Zhang, J. 2004, MNRAS, 354, 811

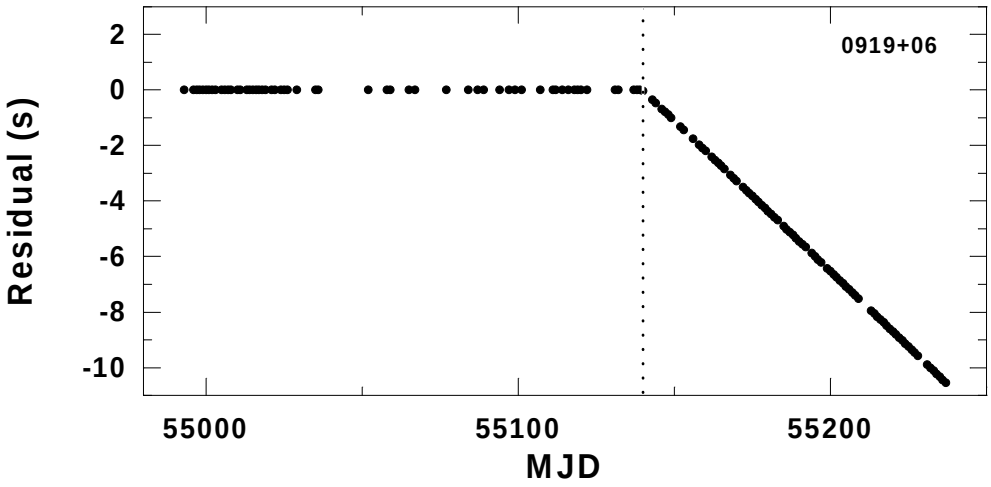

Fig. 1.— Timing residuals for the large glitch that occurred in the period of PSR B0919+06 in 2009 November 5 (MJD 55140). The dotted line indicates the glitch epoch.

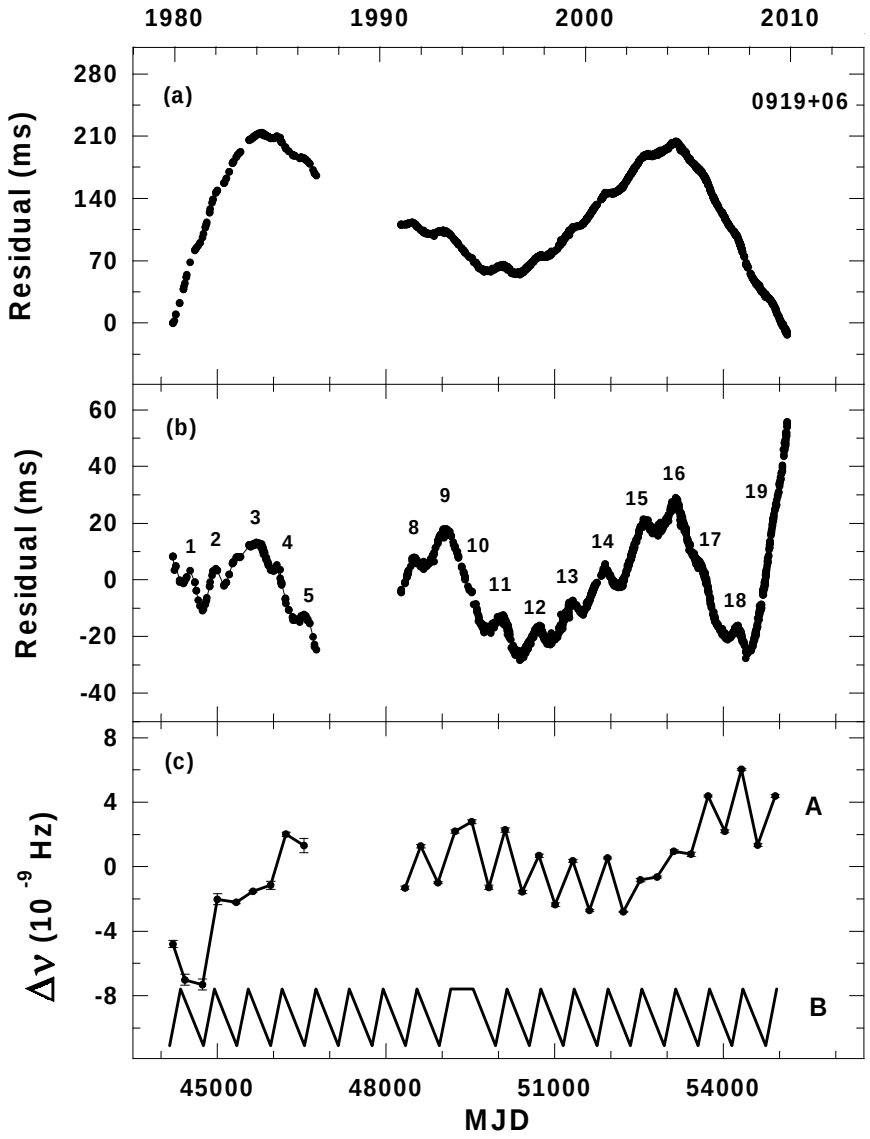

Fig. 2.— Timing behavior of PSR B0919+06 over the 30-year interval from 1979 to 2009. The four-year data gap is seen between 1987 and 1990. (a) The timing residuals after subtraction of the polynomial for ν, $\dot{\nu}$, and $\ddot{\nu}$ for all the pulse arrival times. The residual curve shows the slight short-term cyclical structure. (b) The timing residuals after subtraction of the polynomial for ν and three frequency derivatives. The short-term cyclical structure contains 19 cycles with spacing of maxima of about 600 days. (c) The curve A displays the frequency residuals $\Delta\nu$ relative to the timing model 1979–2009. It is seen that the signature of the $\Delta\nu$ changes has a sawtooth-like character. The curve B is the model sawtooth-like curve that shows how cyclical changes in the rotation frequency could look if the pulsar's rotation was described by a simple spin-down model over the 1979-2009 interval.

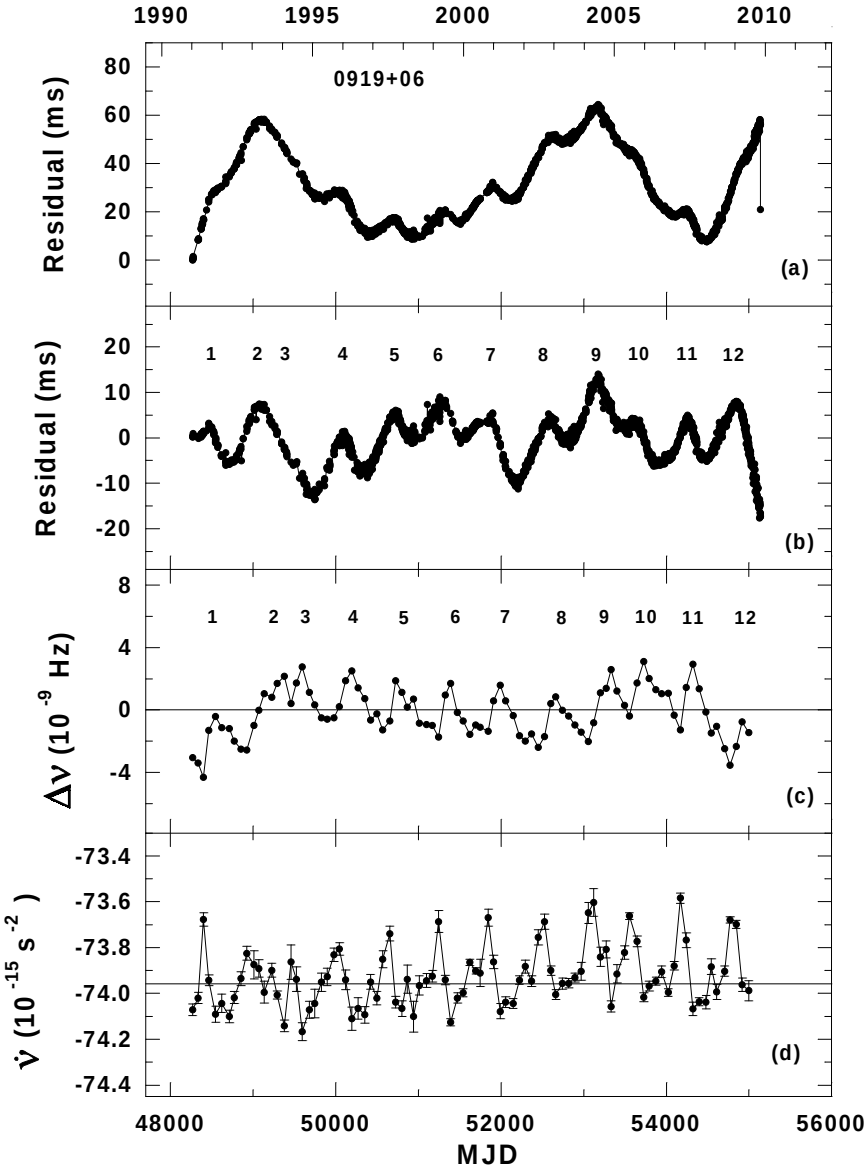

Fig. 3.— Timing behavior of PSR B0919+06 between 1991 and 2009. (a) The timing residuals after subtraction of the polynomial for ν and two frequency derivatives. The last point in the residual curve indicates the large glitch of 2009 November. The slight cyclical structure is clearly seen in the residual curve. (b) The timing residuals after subtraction of the polynomial for ν and five frequency derivatives. The clear cyclical structure contains 12 cycles with the amplitudes of $\sim$ 10 ms and the spacing of maxima of $\sim$ 600 days. (c) The frequency residuals relative to the timing model 1991–2009. Slow oscillations in $\Delta\nu$ look like a continuous sequence of 12 glitch-like events. (d) The changes in the frequency first derivative $\dot{\nu}$ with time. The peaks of $\Delta\dot{\nu}$ define the steepness of the front in $\Delta\nu$.

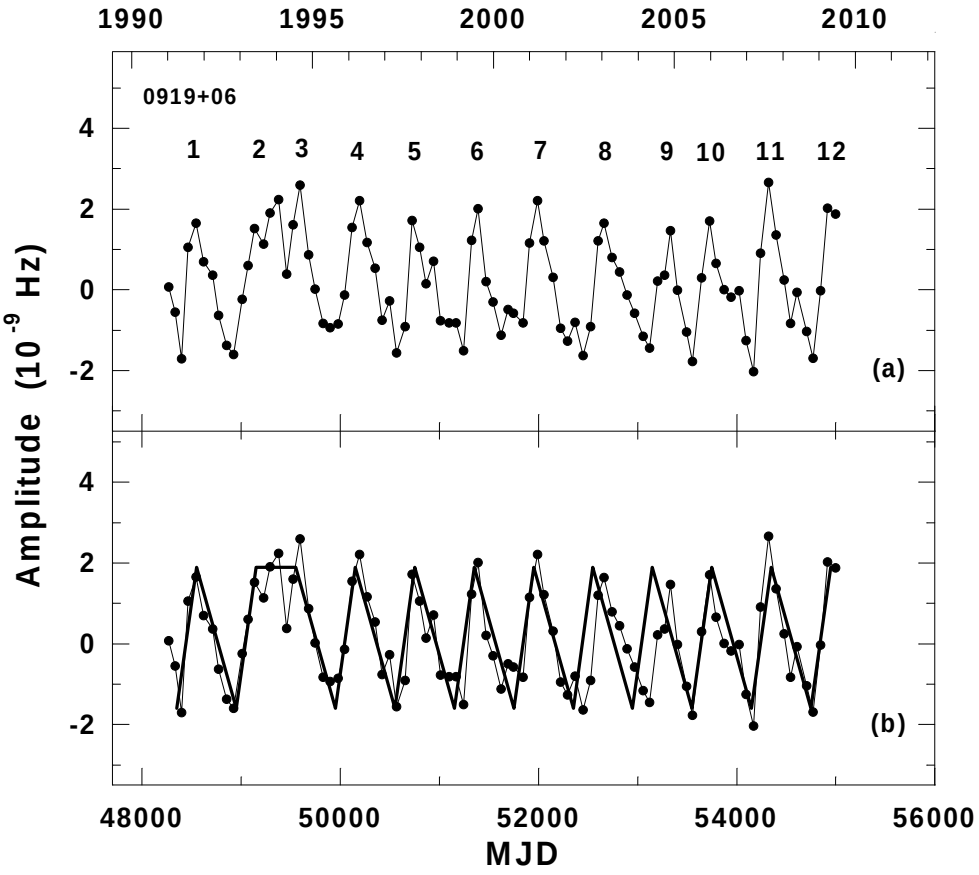

Fig. 4.— Shapes of 12 successive slow glitches observed over the interval 1991–2009. (a) The adjusted set of the $\Delta\nu$ cycles describing the shapes of 12 successive slow glitches. (b) The model sawtooth-like curve with a period of 600 days (marked by the bold line) is superimposed on a sequence of the slow glitches, plotted as in the top panel (a). It is seen that the model sawtooth-like function approximates very well a sequence of the slow glitches observed.

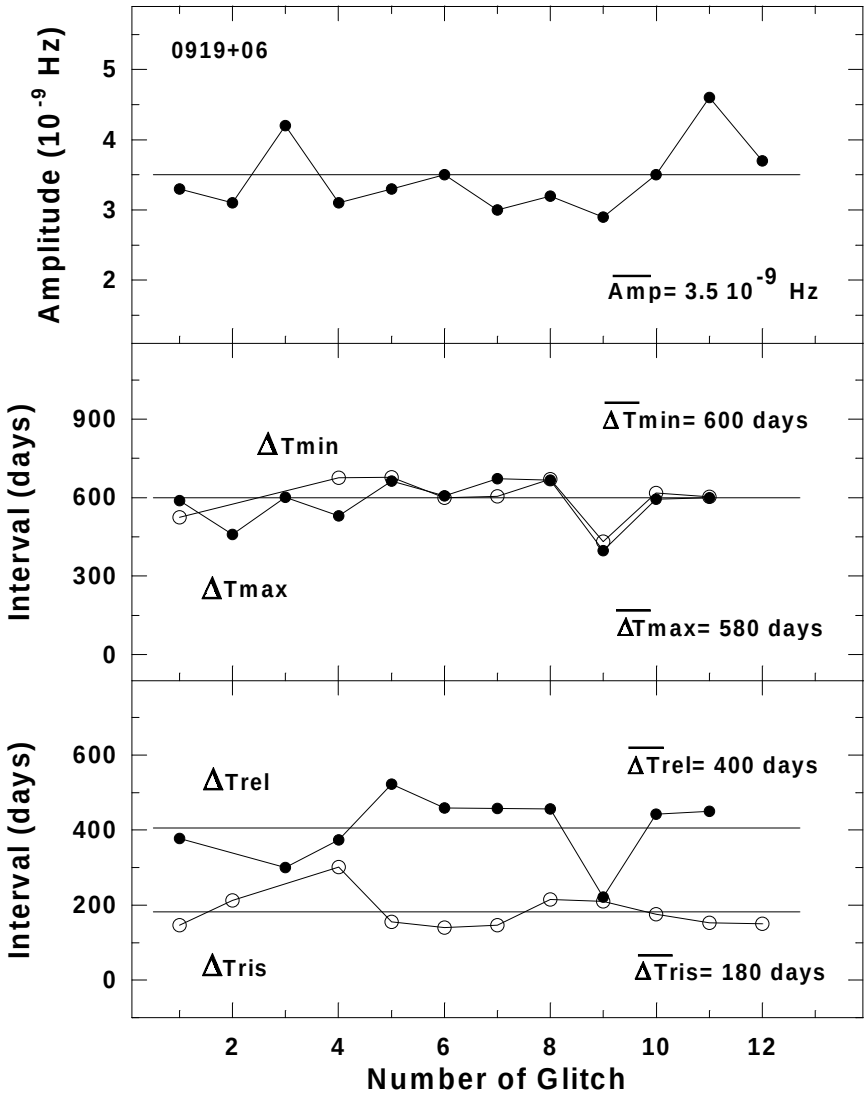

Fig. 5.— Relation between the parameters of 12 slow glitches and the glitch number. The top panel presents a relation between the glitch amplitude and the glitch number. All the slow glitches have approximately an identical amplitude. Its average magnitude equals $\sim 3.5 \times 10^{-9}$ Hz. The mean panel presents a relation between the time interval ΔT_{max} between glitches and the time interval ΔT_{min} between the minimal points of the $\Delta\nu$ cycles and the glitch number. Their average magnitudes equal ~ 580 and ~ 600 days, respectively. The bottom panel presents a relation between the relaxation time interval ΔT_{rel} and the rise time interval ΔT_{ris} and the glitch number. Their average magnitudes equal ~ 400 and ~ 180 days, respectively. The derived average parameters indicate that all the slow glitches have similar properties.

Table 1. The Glitch Parameters for PSR B0919+06

Glitch Parameters	Values
Pre-glitch parameters	
MJD range	54892–55139
ν (Hz)	2.32219343204(6)
$\dot{\nu}$ ($10^{-15}\,s^{-2}$)	-73.931(6)
Epoch (MJD)	54892.8436
RMS Timing Residual (ms)	0.6
Post-glitch parameters	
MJD range	55140–55254
ν (Hz)	2.3221947716(7)
$\dot{\nu}$ ($10^{-15}\,s^{-2}$)	-73.43(8)
Epoch (MJD)	55140.1604
RMS Timing Residual (ms)	0.9
Glitch parameters	
$\Delta\nu/\nu\,(10^{-9})$	1257.1(3)
$\Delta\dot{\nu}/\dot{\nu}\,(10^{-3})$	-7(1)
Epoch (MJD)	55139.8(1)

Table 2. The Rotation Parameters for PSR B0919+06

Parameter	Model 1979–2009	Model 1991–2009
MJD range	44210–55139	48267–55139
ν (Hz)	2.32226169326(9)	2.32223575479(4)
$\dot{\nu}$ ($10^{-15}\,s^{-2}$)	-74.0527(5)	-74.0211(4)
$\ddot{\nu}$ ($10^{-25}\,s^{-3}$)	1.908(13)	3.245(12)
Epoch (MJD)	44210.5817	48266.9832
RMS Timing Residual (ms)	57	15

Table 3. The Observed Parameters for a Sequence of 12 Slow Glitches Revealed in PSR B0919+06 Between 1991 and 2009 (see Figure 4(a))

No.	T_{min} (MJD)	$\Delta\nu_{min}$ (10^{-9} Hz)	T_{max} (MJD)	$\Delta\nu_{max}$ (10^{-9} Hz)	$\Delta\nu_g$ (10^{-9} Hz)	ΔT_{max} (days)	ΔT_{min} (days)	ΔT_{ris} (days)	ΔT_{rel} (days)
1	48398	-1.7	48545	1.6	3.3	589	524	147	377
2	48922	-1.6	49134	1.5	3.1	459	–	212	–
3	–	–	49593	2.6	4.2	601	–	–	300
4	49893	-0.9	50194	2.2	3.1	529	675	301	374
5	50568	-1.6	50723	1.7	3.3	663	678	155	523
6	51246	-1.5	51386	2.0	3.5	606	599	140	459
7	51845	-0.8	51992	2.2	3.0	672	604	147	457
8	52449	-1.6	52664	1.6	3.2	666	671	215	456
9	53120	-1.4	53330	1.5	2.9	396	431	210	221
10	53551	-1.8	53726	1.7	3.5	594	617	175	442
11	54168	-2.0	54320	2.6	4.6	600	602	152	450
12	54770	-1.7	54920	2.0	3.7	–	–	150	–

Note. — In column order, the table gives the glitch number; epoch of the point T_{min}, which corresponds to the minimum deviation of $\Delta\nu_{min}$; epoch of the point T_{max}, which corresponds to the maximum deviation of $\Delta\nu_{max}$; the glitch amplitude $\Delta\nu_g = \Delta\nu_{max} + |\Delta\nu_{min}|$; the time interval to the next glitch ΔT_{max}; the time interval between the minimal points of the $\Delta\nu$ cycle ΔT_{min}; the rise time interval $\Delta T_{ris} = T_{max} - T_{min}$; the relaxation time interval after the glitch $\Delta T_{rel} = T_{min} - T_{max}$.

Table 4. The Parameters for a Model Sawtooth-Like Curve Approximating a Sequence of 12 Slow Glitches Observed (see Figure 4(b))

No.	T_{min} (MJD)	$\Delta\nu_{min}$ (10^{-9} Hz)	T_{max} (MJD)	$\Delta\nu_{max}$ (10^{-9} Hz)
1	48350	-1.6	48550	1.9
2	48950	-1.6	49150	1.9
3	–	–	49550	1.9
4	49950	-1.6	50150	1.9
5	50550	-1.6	50750	1.9
6	51150	-1.6	51350	1.9
7	51750	-1.6	51950	1.9
8	52350	-1.6	52550	1.9
9	52950	-1.6	53150	1.9
10	53550	-1.6	53750	1.9
11	54150	-1.6	54350	1.9
12	54750	-1.6	54950	1.9

Note. — In column order, the table gives the glitch number; epochs of the points T_{min}, which correspond to the minimum deviations of $\Delta\nu_{min}$; epochs of the points T_{max}, which correspond to the maximum deviations of $\Delta\nu_{max}$. The glitch amplitude equals 3.5×10^{-9} Hz, $\Delta T_{ris} = 200$ days, and $\Delta T_{rel} = 400$ days.

Table 5. The Parameters for the Pulsars Showing Slow Glitches

PSR	ν (s^{-1})	$\dot{\nu}$ ($10^{-15}s^{-2}$)	$\ddot{\nu}$ ($10^{-25}s^{-3}$)	τ (years)	B (G)
B1642−03	2.579	-11.84	0.02	3.4×10^6	8.3×10^{11}
B0919+06	2.322	-74.05	1.90	5.0×10^5	2.5×10^{12}
B1822−09	1.300	-88.59	9.00	2.3×10^5	6.4×10^{12}